**PREPARED FOR THE U.S. DEPARTMENT OF ENERGY,
UNDER CONTRACT DE-AC02-76CH03073**

PPPL-3508
UC-70

PPPL-3508

Role of Zonal Flow in Turbulent Transport Scaling

by

Z. Lin, T.S. Hahm, J.A. Krommes, W.W. Lee, J. Lewandowski,
H. Mynick, H. Qin, G. Rewoldt, W.M. Tang, R. White

November 2000

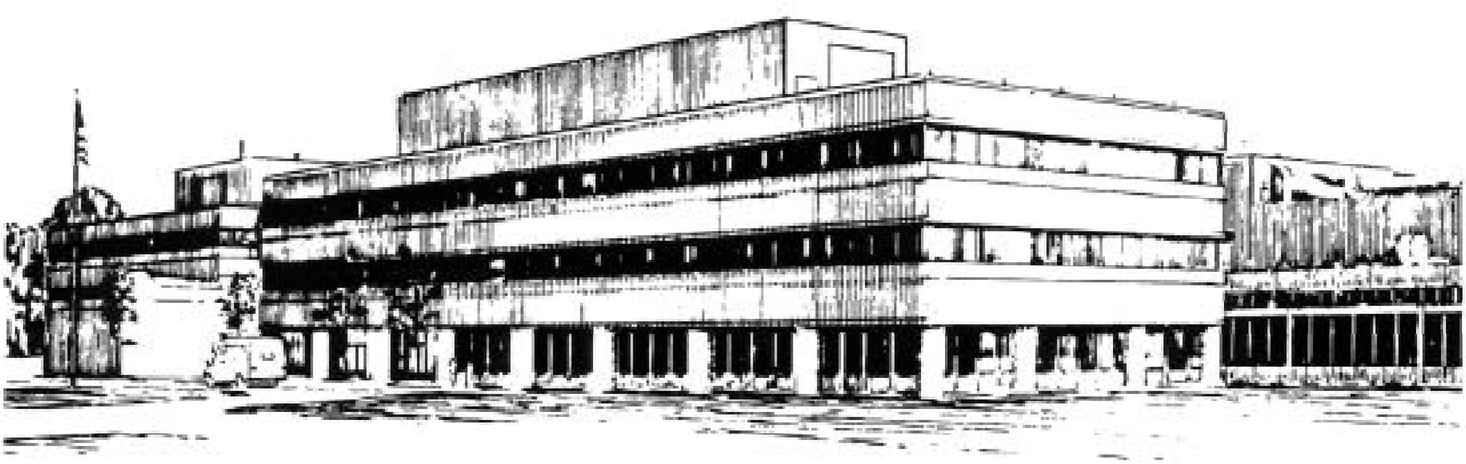

**PRINCETON PLASMA PHYSICS LABORATORY
PRINCETON UNIVERSITY, PRINCETON, NEW JERSEY**

Role of Zonal Flow in Turbulent Transport Scaling

Z. Lin, T. S. Hahm, J. A. Krommes, W. W. Lee, J. Lewandowski,
H. Mynick, H. Qin, G. Rewoldt, W. M. Tang, R. White

Princeton Plasma Physics Laboratory, Princeton, NJ 08543, USA
E-mail: zlin@pppl.gov

October 17, 2000

Abstract

Transport scalings with respect to collisionality (ν^*) and device size (ρ^*) are obtained from massively parallel gyrokinetic particle simulations of toroidal ion-temperature-gradient (ITG) turbulence in the presence of zonal flows. Simulation results show that ion thermal transport from electrostatic ITG turbulence depends on ion–ion collisions due to the neoclassical damping of self-generated $\mathbf{E} \times \mathbf{B}$ zonal flows that regulate the turbulence. Fluctuations and heat transport levels exhibit bursting behavior with a period corresponding to the collisional damping time of poloidal flows. Results from large-scale full torus simulations with device-size scans for realistic parameters show that Bohm-like transport can be driven by microscopic scale fluctuations in the ITG turbulence with isotropic spectra. These simulation results resolve some apparent physics contradictions between experimental observations and turbulent transport theories.

1 Introduction

Transport scalings with respect to collisionality (ν^*) and device size (ρ^*) are obtained from massively parallel gyrokinetic particle simulations of electrostatic toroidal ion-temperature-gradient (ITG) turbulence in the presence of zonal flows. Zonal flows develop spontaneously due to nonlinear effects and, in turn, regulate the turbulence through shear decorrelation. Our simulation results show that zonal flow plays a central role in transport scaling and resolve some apparent physics contradictions between experimental observations and turbulent transport theories. The fact that the nonlinear processes (which generate zonal flows) rather than linear quantities (e.g., growth rate γ or mode spectrum $k_\perp$) determine the scaling of the ion heat conductivity places considerable limitations on the applicability of most existing transport models that are based on an oversimplified $\gamma/k_\perp^2$ type mixing length rule.

These full torus nonlinear simulations with realistic plasma parameters covering disparate spatial and temporal scales only became feasible with the implementation of efficient global field-line-following magnetic coordinates and were enabled by access to the dramatically increasing power of massively parallel computers. The gyrokinetic toroidal code (GTC) [1] with its general geometry capability has also been applied to the assessment of transport properties of compact stellarators and spherical tori.

Ion thermal transport in the core region of a tokamak plasma is believed to arise from electrostatic pressure-gradient driven microinstabilities [2]. In most previous studies, ion-ion collisions have been assumed to have little or no effect on the microinstabilities most likely to be responsible for the ion thermal transport, such as ion-temperature-gradient (ITG) modes. This is because the temperature in present day major tokamak core plasmas is so high that the ion-ion collision frequency is much smaller than the characteristic frequency of the ITG mode (e.g., linear growth rate or nonlinear decorrelation rate, which is of the order of the ion diamagnetic frequency). Consequently, most theory-based ion thermal diffusivities do not contain explicit dependence on the ion-ion collisionality [3].

However, there is some experimental evidence of collisional effects on the core turbulent transport, despite the difficulty in isolating collisional effects by varying the collisionality while keeping other dimensionless parameters constant. A recent transport scaling study on DIII-D core plasmas [4] showed that one-fluid (including both ions and electrons) thermal diffusivity χ_{eff} strongly depends on collisionality in the H-mode, and is almost independent of collisionality in the L-mode. Transport analysis [5] in C-Mod H-mode plasmas resulted in approximately a linear dependence of χ_{eff} on $\nu^* \equiv \epsilon^{-3/2}\nu_{ii}qR_0/v_i$ with q the safety factor, R_0 the major radius, v_i the ion thermal speed, ϵ the inverse aspect ratio and ν_{ii} the ion-ion collision frequency.

Our massively parallel gyrokinetic particle simulations show [6] that the ion thermal transport from electrostatic ITG turbulence depends on ion–ion collisions for representative tokamak core H-mode plasma parameters. The collisionality dependence of the turbulent transport comes from the neoclassical damping of self-generated $\mathbf{E} \times \mathbf{B}$ zonal flows. These zonal flows [7], which are linearly stable $k_\parallel = 0$ modes, are nonlinearly driven [8, 9] by the flux-surface-averaged, radially local current modulations and are mainly in the poloidal direction for high aspect ratio devices. The shear decorrelation [10, 11] by these small scale flows results in the reduction of turbulence and transport. Since the turbulence is regulated by zonal flows, the turbulent transport can depend on ion-ion collisions which damp poloidal flows through the neoclassical effects. The results from full torus simulations with a momentum- and energy-conserving Fokker–Planck collision operator are consistent with the experimental observation that the collisionality dependence of transport is much more pronounced in the enhanced confinement regime (where turbulence is expected to be weaker) than that of typical L-mode plasmas. Furthermore, the fluctuations and heat transport in these simulations exhibit bursting behavior with a period corresponding to the collisional damping time of poloidal flows. This is consistent with the observation in TFTR core plasmas [12] of density fluctuations bursting with a period (~ 3 ms) which is close to the collisional flow damping time calculated from experimental plasma parameters.

Most ITG turbulent transport theories and models assume small scale fluctuations and consequently predict gyro-Bohm scaling. However, in previous full torus gyrokinetic simulations with zonal flow artificially suppressed, Bohm-like transport scaling was observed due to radially elongated turbulent eddies resulting from linear global modes. Our more realistic simulations with zonal flow self-consistently included found [1] that the random shearing of ITG turbulence by the zonal flow results predominantly in the reduction of the radial correlation length and subsequently in the turbulence level. The fluctuations are nearly isotropic in the radial and poloidal directions. This motivated us to carefully study ρ^* ($\rho^* = \rho_i/a$ with ρ_i the ion gyroradius and a the minor radius) scaling with self-generated zonal flow using our large-scale simulations with device-size scans. Simulation results show that ITG transport can deviate from the gyro-Bohm scaling even with isotropic spectra. This is consistent with tokamak dimensionless scaling studies which found that ion transport and energy confinement time exhibit Bohm-like behavior [13] while fluctuation characteristics suggest gyro-Bohm scaling [14].

2 $\nu*$ scaling

In toroidal geometry, an initial source of zonal flows is damped by the collisionless transit time magnetic pumping effects followed by a slowly damped geodesic acoustic mode (GAM) [15] oscillation. Rosenbluth and Hinton [16] have pointed out the existence of a residual flow which survives this linear collisionless damping process in the banana regime. This undamped component of poloidal flows plays a key role in determining the turbulent transport level in nonlinear simulations; thus its long time behavior must be treated accurately. This residual flow is eventually damped out by ion-ion collisions and, possibly, by nonlinear effects. In the present work, the GTC linear simulation of the collisional flow damping is benchmarked with an analytical calculation [17]. In this simulation, we solve a toroidal gyrokinetic equation [18, 19] with a flux-surface-averaged source which introduces an initial perturbation of the poloidal flow. Without collisions, an asymptotic residual of this flow develops and its level measured from the simulation agrees with the theoretical prediction. When ion-ion collisions are included, this residual flow is slowly damped. The collisional decay of the flow perturbation in the gyrokinetic simulation agrees [1] well with the analytical calculation [17] (see below for plasma parameters). The analytical theory only deals with time scales longer than the ion bounce period; therefore it does not describe the transient processes associated with magnetic pumping and GAM oscillations. Most of the collisional damping occurs through the friction force between trapped and passing particles [17]. The effective damping time measured from the simulation is very close to the theoretical prediction of $\tau_d = 1.5\epsilon\tau_{ii}$, where τ_{ii} is the ion-ion collision time. A like-species Lorentz operator is used in this simulation for comparison with the theory. In the following nonlinear simulations, we use a momentum and energy conserving Fokker-Planck operator which has been rigorously benchmarked for neoclassical transport [20].

With validity checks completed, the GTC was next applied to full torus nonlinear simulations of ITG turbulence. These simulations used representative parameters of DIII-D tokamak H-mode core plasmas which have a peak ion temperature gradient at $r = 0.5a$ with the following local parameters [21]: $R_0/L_T = 6.9$, $R_0/L_n = 2.2$, $q = 1.4$, $\hat{s} \equiv (r/q)(dq/dr) = 0.78$, $T_e/T_i = 1$, $\epsilon = 0.18$, and $\nu^* = 0.045$. Here L_T and L_n are the temperature and density gradient scale lengths, respectively, T_i and T_e are the ion and electron temperatures. The size of the plasma column is $a = 160\rho_i$ where ρ_i is the thermal ion gyroradius measured at $r = 0.5a$. The simplified physics model included: a parabolic q profile, a pressure gradient profile $exp\{-[(r-0.5a)/0.3a]^6\}$, a circular cross section, no impurities, and an adiabatic electron response [22] with $\delta n_e/n_0 = e(\phi - \langle\phi\rangle)/T_e$, where $\langle\cdots\rangle$ represents the flux surface average. These global simulations used fixed boundary conditions with $\phi = 0$ enforced at $r < 0.1a$ and $r > 0.9a$. ITG modes are unstable with these plasma parameters and have a linear threshold of $R_0/L_T = 4$ [21]. The parameter R_0/L_T represents the strength of the turbulence drive. We scan R_0/L_T to assess sensitivity of the collisional effects to the proximity to ITG marginality.

For a strong ITG drive of $R_0/L_T = 6.9$, both turbulence and zonal flows saturate and reach steady state in collisionless simulations. When realistic ion-ion collisions with $\nu^* = 0.045$ are included in the simulation, the steady state ion heat conductivity χ_i is increased by about one half from the collisionless value. The saturated zonal flow level decreases due to collisions. Meanwhile, the change in linear growth rate is negligible. Furthermore, when zonal flows are not included in the simulations, collisions have little effect on the turbulent transport. We therefore conclude that the enhancement of transport by collisions in the presence of zonal flows is through the neoclassical damping of zonal flows. When the turbulence drive R/L_T is reduced, nonlinear flow damping becomes insignificant. The collisionless system can undergo a transition to a flow-dominated state where zonal flows generated from the initial growth of turbulence completely suppress the turbulence and transport [8, 21]. In this paper, we characterize this regime as the weak turbulence regime. Collisionless nonlinear flux-tube gyrokinetic simulations for the same plasma parameters have found [21] that, for $R/L_T = 4$ to 6, no transport is produced even though the system is linearly unstable to ITG modes. However, collisions can remove this nonlinear upshift of the critical gradient by slowly damping zonal flows. The ion thermal transport level will then strongly depend on the collision frequency. Since most of the plasma volume of the representative DIII-D discharge has $R/L_T < 6$, it should be emphasized that the physics discussed here is relevant to many tokamak experiments.

We now reduce the turbulence drive to $R/L_T = 5.3$ in our nonlinear simulations. The ITG mode is unstable with linear growth rate $\gamma = 0.072 v_i/L_n$ and real frequency $\omega_r = -0.29 v_i/L_n$ at $k_\theta \rho_i = 0.35$. We scan the ion-ion collision frequency upward from the experimental value to facilitate studies of the long term collisional effects on the zonal flow dynamics. Again, the collisional effect on the linear growth rate of the ITG mode is less than 1% for all the collision frequencies. In the collisionless simulation, the saturated heat flux decreases to an insignificant level due to shearing effects of zonal flows which reach a steady state level. When collisions are introduced, zonal flows are damped and a finite transport level is obtained. As we increase the collision frequency without changing other parameters, we observe an increase of the time-averaged χ_i without a tendency toward saturation for the whole scan range of collision frequencies, which is up to 8 times the experimental value. Fig. 1 shows that the ion heat conductivity sensitively depends on the collision frequency in this weak turbulence regime. This collisionality-dependence of the turbulent transport implies that an accurate treatment of the linear poloidal flow damping [16, 17] in nonlinear simulation codes is essential in predicting the transport levels.

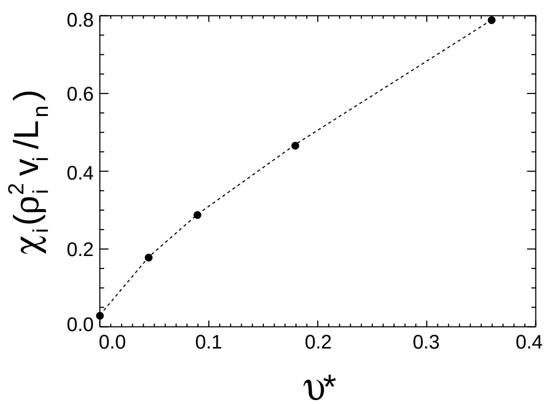

Figure 1: Ion heat conductivity in nonlinear gyrokinetic simulations with $R/L_T = 5.3$ vs. the ion-ion collision frequency.

The simulation time history for the case $\nu^* = 0.09$ is shown in Fig. 2. The ITG instabilities evolve from a linear phase of exponential growth to a nonlinear stage in which zonal flows are generated. When the effective shearing rate [23], or root mean square shearing rate [8] of zonal flows exceeds the ambient turbulence decorrelation rate which can be approximated by the ITG linear growth rate [24], the ITG turbulence and associated transport are significantly reduced. Zonal flows are then slowly damped by the ion-ion collisions. When the effective shearing rate is below the growth rate, the ITG turbulence grows again and drives zonal flows. These turbulence-zonal flows interactions modulated by collisions result in a cyclic, bursting behavior of fluctuations, transport and zonal flows. From a scan of the collision frequency, we observe that the bursting period is of the order of the collisional damping time of the zonal flows, τ_d.

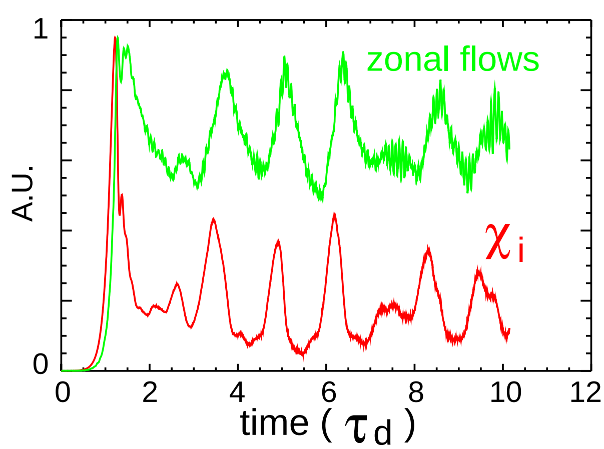

Figure 2: Time history in nonlinear gyrokinetic simulations for zonal flow amplitude and ion heat conductivity.

In a weak turbulence system, the turbulence-zonal flow-turbulence interaction is the dominant triad [8, 9] and the zonal flows are damped by collisions. The ITG modes are saturated by the zonal flow shear decorrelation. On the other hand, the zonal flows saturate when the generation rate of the modulational instability is balanced by the collisional damping rate. This analysis of the model weak turbulence system [8, 9] yields $(\delta\phi)^2 \propto \nu_{ii}$ in steady state. Since $\chi_i \propto (\delta\phi)^2$ is expected when the turbulence drive is weak, one would expect $\chi_i \propto \nu_{ii}$, which is qualitatively consistent with the results from our first-principle gyrokinetic simulations. As we increase the collision frequency $\nu_{ii} \rightarrow \infty$, while keeping the linear growth rate finite, one would expect to recover the usual strong turbulence scaling. Transition from weak to strong turbulence regimes, however, can be complicated by the collisional detrapping of the resonant particles that are trapped by the waves [25].

3 $\rho*$ scaling

$\rho*$ scaling of anomalous transport enables extrapolation of confinement properties from existing devices to future machines.In the absence of a fundamental, first-principle turbulence theory, a heuristic, mixing length rule is often utilized in obtaining such scaling theoretically. Most turbulence theories and local (or flux-tube) direct simulations assume fluctuation on a microscopic scale length ($k_\perp \rho_i \sim 1$) and predict gyro-Bohm transport. However, trends from experimental observations have been more complicated and can include gyro-Bohm, Bohm, or other scaling. Global (full torus) direct simulations have been used to resolve this puzzle. Previous global gyrokinetic simulations of toroidal ITG modes with zonal flow suppressed observed Bohm-like transport driven by radially elongated eddies of linear global modes. However, more realistic simulations with zonal flows self-consistently included show [1] that these global mode structures are destroyed by the shearing action of zonal flows and the turbulent eddy size becomes independent of device size (Fig. 3).

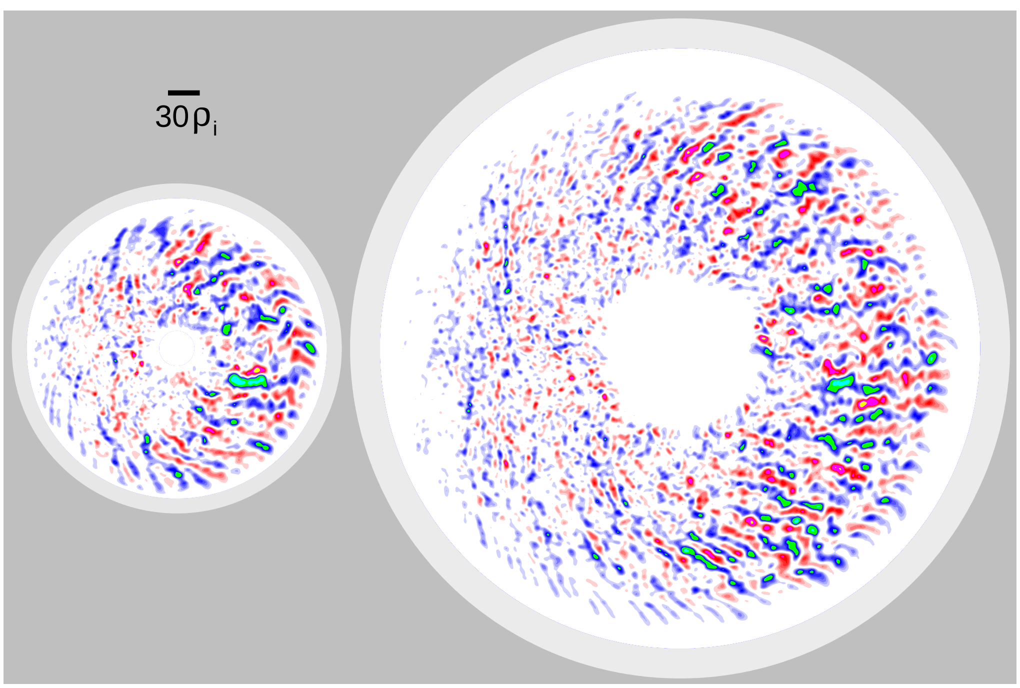

Figure 3: Poloidal contour plots of fluctuation potential in nonlinear state showing turbulence eddy size independent of device size.

This observation motivates us to systematically scan device size while keeping all other plasma parameters fixed in nonlinear simulations. To minimize the collisional effects in this device size scan, we use a stronger drive for the ITG instability with $R/L_T = 6.9$ and keep all other plasma parameters the same as those specified in Sec. 2. The simulation of device size $a = 400\rho_i$ uses 200 million gyrocenters. The numerical resolution in such a simulation with field-line following magnetic coordinates is equivalent to that of a simulation with conventional coordinates using more than 2 billion gyrocenters. The radial power spectra of the fluctuating potential (excluding the zonal flow mode which does not cause transport) are indeed observed to be similar for all device sizes (see Fig. 4). In contrast, when zonal flows are suppressed in the simulation, the radial spectra is narrower (dominant by low k_r components) for larger device sizes. Based on mixing length estimates, such small scale fluctuations should drive gyro-Bohm transport.

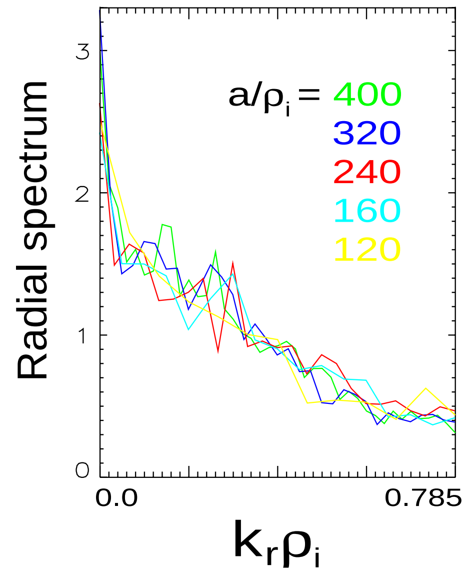

Figure 4: radial spectra of potential for various device sizes

Surprisingly, the ion heat conductivity in this scan exhibits Bohm-like scaling for device size $a > 160\rho_i$. This observation is consistent with recent dimensionless scaling studies on the DIII-D tokamak which found that ion transport and energy confinement time exhibit Bohm-like behavior while fluctuation characteristics suggest gyro-Bohm scaling [14]. How can small scale fluctuations drive Bohm-like transport? Possible mechanisms responsible for such scaling include: (a) the existence of large transport events where a heat pulse propagates ballistically; (b) wave transport where the wave extracts energy from ions in the hot region and deposits it back to ions in the cold region; and (c) profile ($\omega*$) variation effects due to finite device size in simulations. In the following, we examine each of them.

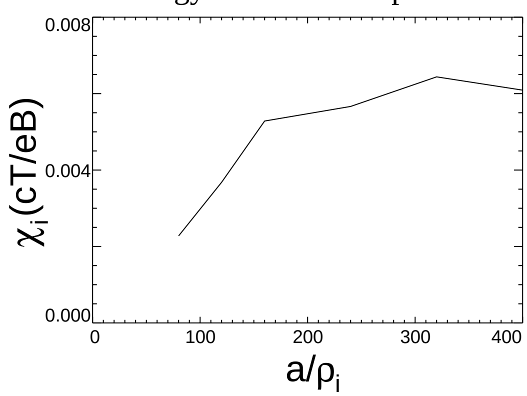

Figure 5: Ion heat conductivity vs. device size

First we measure the radial diffusion of test particles (passive particles that do not affect the turbulence). After nonlinear saturation, 6 million test particles are initiated around $r = 0.5a$ with a uniform poloidal distribution. The probability distribution function of radial displacement after about 10 eddy turnover times is measured and is found to be very close to a Gaussian (Fig. 6). Further examination of the deviation from Gaussian reveals no singular structure in either pitch angle or energy space. This indicates that there is no sharp resonance in wave-particle interactions. Since the radial motion of test particles is diffusive rather than ballistic, the wave does not trap and convect the particles, but only scatters the particle orbits. With the apparent absence of a large transport event over this simulation time, longer (macroscopic) time scale simulations need to be performed.

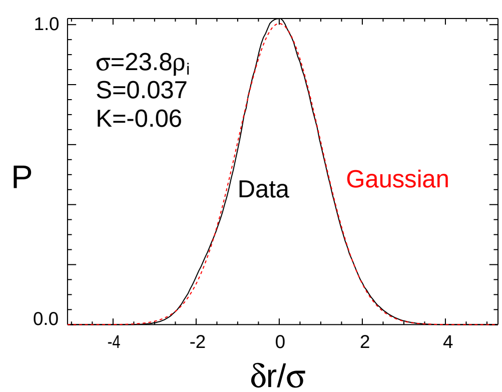

Figure 6: Probability density function of test particle radial displacement (black) vs. Gaussian function (red).

Since the test particle radial motion is diffusive, we can calculate ion heat conductivity based on the random walk model of test particle heat flux, Q, due to the energy-dependent diffusivity $D = \sigma^2/2t$, $Q = -\int \frac{1}{2} v^2 D \partial f/\partial r d^3 v$. We also measure the self-consistent heat flux, $Q = \int \frac{1}{2} v^2 \delta v_{E\times B} \delta f d^3 v$. We found that the test particle heat flux is very close to the self-consistent heat flux (Fig. 7), and that wave transport does not play a significant role. We conclude that the heat flux is carried by the radial diffusion of particles. Finally, we found that the fluctuation amplitude (excluding zonal flows) scales as $\delta v_{E\times B} \propto V_{dia}/\sqrt{\rho *}$. This is inconsistent with mixing length estimate which predicts $\delta v_{E\times B} \propto V_{dia}$. It also indicates that $E \times B$ trapping does not play a dominant role in the nonlinear decorrelation (otherwise the heat conductivity would scale as $\sqrt{\rho *}$). In fact the effective correlation time (defined by $\tau = D/\delta v_{E\times B}^2$) scales as $\tau \sim 1/\omega *$, consistent with the scaling of the zonal flow shearing rate. Note that the observed $\rho *$ scaling of $\delta v_{E\times B}$ is not physical in a larger device ($\rho * \rightarrow 0$) because the fluctuating velocity cannot become arbitrarily larger than the diamagnetic drift velocity, which is the characteristic velocity of the system. Therefore the current $\delta v_{E\times B}$ scaling may be a result of sharp profile variation of $\omega *$ in the relatively small size device (even though the simulation size is larger than most existing machines). Work is underway for simulation of a much larger size device (reactor scale $a = 1000\rho_i$), where the profile variation effect is expected to be weaker, to determine whether the profile variation is responsible for the Bohm-like transport.

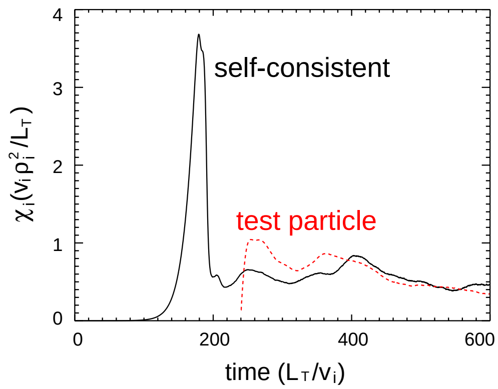

Figure 7: Ion heat conductivity measured self-consistently (black) and calculated through test particle diffusion,

4 Conclusions

Transport scalings with respect to collisionality (ν^*) and device size (ρ^*) are obtained from massively parallel gyrokinetic particle simulations of electrostatic toroidal ion-temperature-gradient (ITG) turbulence in the presence of zonal flows. Simulation results show that ion thermal transport from electrostatic ITG turbulence depends on ion–ion collisions and that fluctuations and heat transport level exhibit bursting behavior. Results from large-scale full torus simulations with device-size scans for realistic parameters show that Bohm-like transport can be driven by microscopic scale fluctuations with isotropic spectra. Our simulation results resolve some apparent physics contradictions between experimental observations and turbulent transport theories. Furthermore, the fact that the change of the ion heat conductivity χ_i with collision frequency cannot be attributed to the change in the linear growth rate γ or the mode spectrum $k_\perp$ places considerable limitations on the applicability of existing transport models that are based on an oversimplified $\gamma/k_\perp^2$ type mixing length rule.

References

[1] Z. Lin, T. S. Hahm, W. W. Lee, W. M. Tang, and R. B. White, *Science* **281**, 1835 (1998).

[2] W. M. Tang, *Nucl. Fusion* **18**, 1089 (1978).

[3] J. W. Connor and H. R. Wilson, *Plasma Phys. Contr. Fusion* **36**, 719 (1994).

[4] C. C. Petty and T. C. Luce, *Phys. Plasmas* **6**, 909 (1999).

[5] M. Greenwald, *et al.*, *Plasma Phys. Contr. Fusion* **40**, 789 (1998).

[6] Z. Lin, T. S. Hahm, W. W. Lee, W. M. Tang, and P. H. Diamond, *Phys. Rev. Lett.* **83**, 3645 (1999).

[7] A. Hasegawa, C. G. Maclennan, and Y. Kodama, *Phys. Fluids* **22**, 2122 (1979).

[8] P. H. Diamond, et al., in Proceedings of the 17th IAEA Conference on Controlled Fusion and Plasma Physics, Yokahama, Japan, 1998.

[9] Liu Chen, Zhihong Lin, and Roscoe White. *Phys. Plasmas* **7**, 3129 (2000)

[10] H. Biglari, P. H. Diamond, and P. W. Terry, *Phys. Fluids* B **2**, 1 (1990).

[11] T. S. Hahm and K. H. Burrell, *Phys. Plasmas* **2**, 1648 (1995).

[12] E. Mazzucato, *et al.*, *Phys. Rev. Lett.* **77**, 3145 (1996).

[13] F. W. Perkins, *et al.*, *Phys. Fluids B* **5**, 477 (1993).

[14] G. McKee, *et al.*, Transport Task Force workshop, Burlington, Vermont, April 28, 2000.

[15] N. Winsor, *et al.*, *Phys. Fluids* **11**, 2448 (1968).

[16] M. N. Rosenbluth and F. L. Hinton, *Phys. Rev. Lett.* **80**, 724 (1998).

[17] F. L. Hinton and M. N. Rosenbluth, *Plasma Phys. Controlled Fusion* **41**, A653 (1999).

[18] E. A. Frieman and L. Chen, *Phys. Fluids* **25**, 502 (1982).

[19] T. S. Hahm, *Phys. Fluids* **31**, 2670 (1988).

[20] Z. Lin, W. M. Tang, and W. W. Lee, *Phys. Rev. Lett.* **78**, 456 (1997).

[21] A. M. Dimits, *et al.*, *Phys. Plasmas* **7**, 969, 2000.

[22] G. W. Hammett, *et al.*, *Plasma Phys. Contr. Fusion* **35**, 973 (1993).

[23] T. S. Hahm, *et al.*, *Phys. Plasmas* **6**, 922 (1999).

[24] R. E. Waltz, G. D. Kerbel, J. Milovich, *Phys. Plasmas* **1**, 2229 (1994).

[25] W. W. Lee and W. M. Tang, *Phys. Fluids* **31**, 612 (1988).

The Princeton Plasma Physics Laboratory is operated
by Princeton University under contract
with the U.S. Department of Energy.

Information Services
Princeton Plasma Physics Laboratory
P.O. Box 451
Princeton, NJ 08543

Phone: 609-243-2750
Fax: 609-243-2751
e-mail: pppl_info@pppl.gov
Internet Address: http://www.pppl.gov